VIII International Conference on Computational Plasticity
COMPLAS VIII
E. Oñate and D.R.J. Owen (Eds)

DISPERSION AND LOCALISATION IN A STRAIN–SOFTENING MULTIPHASE MEDIUM

René de Borst⋆ and Marie-Angèle Abellan†

⋆Faculty of Aerospace Engineering, TU Delft, 2600 GB Delft, Netherlands, and
LaMCoS, UMR CNRS 5514, I.N.S.A. de Lyon, 69621 Villeurbanne, France
e-mail: R.deBorst@LR.TUDelft.nl, web page: http://www.em.lr.tudelft.nl

† LTDS-ENISE, UMR CNRS 5513, ENISE, 42023 Saint-Etienne, France

Key words: Softening, localisation, dispersion, internal length scale, multiphase media.

Summary. *Dispersion analyses are carried out for a fluid–saturated, one–dimensional continuum. A dispersive wave is obtained, but the associated internal length scale vanishes in the short wave–length limit. Accordingly, upon the introduction of softening, localisation in a zero width will occur and no regularisation is present. This conclusion is corroborated by numerical analyses of wave propagation in a finite one–dimensional bar.*

1 INTRODUCTION

The introduction of strain softening in the constitutive relation for a standard, rate–independent solid normally causes a loss of well-posedness of the initial value problem, cf. [1]. The absence of a *physical* internal length scale causes a *numerical* length scale to be introduced in the computations, typically the distance between two neighbouring grid points, and the solution becomes mesh-dependent.

Physically based internal length scales have been derived for a single–phase media equipped with a rate–dependent [2] or with a gradient–dependent constitutive model [3]. By investigating the possible dispersive properties of wave propagation in strain–softening media, either a cut-off wave number was identified at which loading waves are no longer able to propagate (gradient–dependent case), or, for the rate–dependent case, the damping factor was derived as a function of stiffness, viscosity and mass density for the limiting case of waves with a vanishing wave length (the short wave-length limit).

2 GOVERNING EQUATIONS

For a fluid–saturated, one–dimensional continuum, the balances of momentum and mass read in an incremental format, e.g. [4] for a complete derivation:

$$\frac{\partial \dot{\sigma}_s}{\partial x} + n_f K^{-1}(\dot{v}_f - \dot{v}_s) - \rho_s \frac{\partial \dot{v}_s}{\partial t} - \rho_f \frac{\partial \dot{v}_f}{\partial t} = 0 \tag{1}$$

and

$$\alpha \frac{\partial^2 \dot{v}_s}{\partial x^2} + n_f \left(\frac{\partial^2 \dot{v}_f}{\partial x^2} - \frac{\partial^2 \dot{v}_s}{\partial x^2} \right) - n_f (KQ)^{-1} \left(\frac{\partial \dot{v}_f}{\partial t} - \frac{\partial \dot{v}_s}{\partial t} \right) = 0 \tag{2}$$

They are supplemented by the kinematic relation and the incremental stress–strain relation, which, after combination, read:

$$\dot{\sigma}_s = E^{tan} \frac{\partial \dot{u}_s}{\partial x} \tag{3}$$

with E^{tan} the tangential stiffness modulus of the solid.

3 DISPERSION ANALYSIS

To analyse the characteristics of wave propagation in the two–phase medium defined in the preceding section, a damped, harmonic wave is considered:

$$\begin{pmatrix} \delta\dot{u}_s \\ \delta\dot{u}_f \end{pmatrix} = \begin{pmatrix} A_s \\ A_f \end{pmatrix} \exp\left(\lambda_r t + \mathrm{i}(kx - \omega t)\right) \tag{4}$$

with λ_r representing the damping and ω the angular frequency. Substitution of this identity into eqs (1)–(2), using eq. (3), requiring that a non-trivial solution can be found for the resulting set of homogeneous equations and decomposing into real and imaginary parts leads to:

$$8\lambda_r^3 + 8ak^2\lambda_r^2 + 2(a^2k^2 + b)k^2\lambda_r + (ab - c)k^4 = 0 \tag{5}$$

and

$$\omega^2 = 3\lambda_r^2 + 2ak^2\lambda_r + bk^2 \tag{6}$$

with

$$a = \frac{KQ(\rho_s + (n_f - \alpha)\rho_f')}{\rho_s + \rho_f} \ , \ b = \frac{E^{tan} + \alpha Q}{\rho_s + \rho_f} \ , \ c = \frac{KQE^{tan}}{\rho_s + \rho_f} \tag{7}$$

Evidently, wave propagation is dispersive, since eq. (6) is such that the phase velocity $c_f = \omega/k$ is dependent on the wave number k, cf. [5, 6]. Taking the long wave–length limit in eq. (5), i.e. $k \to 0$, yields $\lambda_r \to 0$. According to eq. (6) and after substitution of eq. (7b), we obtain an explicit expression for the phase velocity:

$$c_f = \frac{\omega}{k} = \sqrt{\frac{E^{tan} + \alpha Q}{\rho_s + \rho_f}} \tag{8}$$

Using Cardano's formulas, eq. (5) can be solved explicitly. For the short wave-length limit, i.e. when $k \to \infty$, we obtain that the discriminant $D \to 0$, which identifies the existence of three real roots for λ_r in this limiting case, two of them being equal. For the single root we obtain that $\lambda_r \to 0$. This implies that this solution has no damping properties and, therefore, gives no regularisation. For the double root we find that $\lambda_r \sim -k^2$. From eq. (6) the expression for the phase velocity then becomes proportional to the wave number, $c_f \sim k$ (please note that for strain softening c_f will normally be imaginary).

In view of eq. (4) and in analogy with a single–phase rate–dependent medium [2], an internal length scale can be defined as:

$$\ell = \lim_{k\to\infty}\left(-\frac{c_f}{\lambda_r}\right) \sim \lim_{k\to\infty} k^{-1} = 0 \tag{9}$$

which indicates that the internal length scale ℓ vanishes in the short wave–length limit.

4 NUMERICAL EXAMPLES

To verify and elucidate the theoretical results of the preceding section, a finite difference analysis has been carried out. The spatial derivatives in eqs (1) and (2) have been approximated with a second–order accurate finite difference scheme. Explicit forward finite differences have been used to approximate the temporal derivatives, which is first-order accurate. The choice for a fully explicit time integration scheme was motivated by the analysis of Benallal and Comi [6], in which they showed that in this case no numerical length scale was introduced in the analysis, apart from the grid spacing. As implied in eqs (1) and (2) the velocities v_s and v_f of the solid skeleton and the fluid have been taken as fundamental unknowns and the displacements have been obtained by integration.

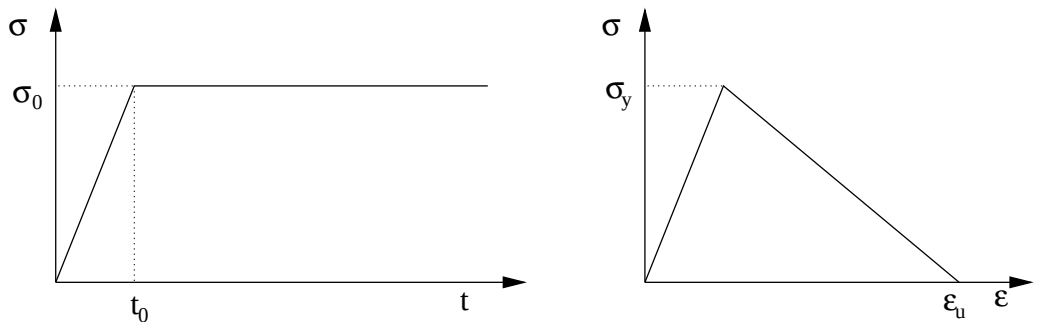

Figure 1: Applied stress as function of time (left) and local stress–strain diagram (right)

.

All calculations have been carried out for a bar with a length $L = 100\ m$. For the solid material, a Young's modulus $E = 20\ GPa$ and an absolute mass density $\rho_s' = 2000\ kg/m^3$ have been assumed. For the fluid, an absolute mass density $\rho_f' = 1000\ kg/m^3$ was adopted and a compressibility modulus $Q = 5\ GPa$ was assumed. As regards the porosity, a value $n_f = 0.3$ was adopted and in the reference calculations $\alpha = 0.6$ and the permeability $K = 10^{-10}\ m^3/Ns$. In all cases, the external compressive stress was applied according to the scheme shown in Figure 1, with a rise time $t_0 = 0.05\ s$ to reach the peak level $\sigma_0 = 1.5\ MPa$. A time step $\Delta t = 0.5\cdot 10^{-3}\ s$ was adopted, which is about half the critical time step for this explicit scheme.

Upon reflection at the right boundary, the stress intensity doubles and the stress in the solid exceeds the yield strength $\sigma_y = 2.5\ MPa$ and enters a linear descending branch with

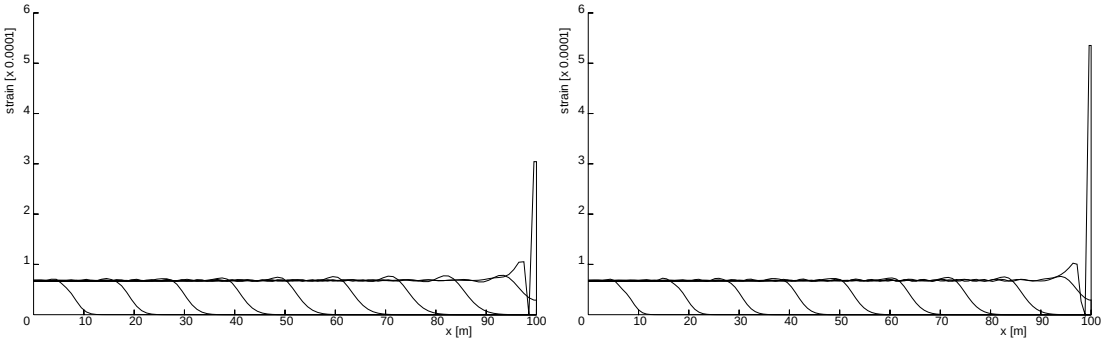

Figure 2: Strain profiles along the bar for 101 (left) and 126 (right) grid points and time step $\Delta t = 0.5 \cdot 10^{-3}\ s$

.

an ultimate strain $\epsilon_u = 1.125 \cdot 10^{-3}$, see Figure 1. Figure 2 (left) shows that a Dirac–like strain distribution develops immediately upon wave reflection. This is logical, since a standard two–phase medium does not have regularising properties. To further strengthen this observation the analysis was repeated with a slightly refined mesh (126 grid points), which resulted in a marked increase of the localised strain (Figure 2 – right), which has been plotted on the same scale as the results of the original discretisation in Figure 2. In [4] it has been shown that also the time step strongly influences the results, cf. [6].

REFERENCES

[1] R. de Borst. Damage, material instabilities, and failure. In *Encyclopedia of Computational Mechanics*. E. Stein, R. de Borst and T.J.R. Hughes (eds). Wiley, Chichester, 2004; Volume 2, Chapter 10.

[2] L.J. Sluys and R. de Borst. Wave propagation and localisation in a rate-dependent cracked medium — Model formulation and one-dimensional examples. *Int. J. Sol. Struct.*, **29:** 2945–2958, 1992.

[3] L.J. Sluys and R. de Borst and H.-B. Mühlhaus. Wave propagation and dispersion in a gradient-dependent medium. *Int. J. Sol. Struct.*, **30:** 1153–1171, 1993.

[4] M.-A. Abellan and R. de Borst. Wave propagation and localisation in a softening two–phase medium. *Comp. Meth. Appl. Mech. Eng.*, accepted for publication.

[5] H.W. Zhang, L. Sanavia and B.A. Schrefler. An internal length scale in dynamic strain localization of multiphase porous media. *Mech. Coh.-frict. Mat.*, **4:** 445–460, 1999.

[6] A. Benallal and C. Comi. On numerical analyses in the presence of unstable saturated porous materials. *Int. Journal Num. Meth. Eng.*, **56:** 883–910, 2003.